The BLAST Cherenkov Detectors

B. Tonguc [a], R. Alarcon [a], T. Botto [c], J. Calarco [b], A. Degrush [d], O. Filoti [b], E. Geis [a], J. Kelsey [c], J. Prince [a], E. Six [a], C. Vidal [c]

[a] *Department of Physics and Astronomy, Arizona State University, Tempe, AZ, USA*

[b] *Department of Physics, University of New Hampshire, Durham, NH, USA*

[c] *MIT-Bates Linear Accelerator Center, Massachusetts Institute of Technology, Middleton, MA, USA*

[d] *Department of Physics, Massachusetts Institute of Technology, Cambridge, MA, USA*

Abstract

We report on the design, construction, and operation of a large array of diffusely reflective aerogel Cherenkov detectors. They are part of the detector instrumentation of the Bates Large Acceptance Spectrometer Toroid (BLAST) at the MIT-Bates Linear Accelerator Center. The Cherenkov detectors are used for particle identification. They are able to discriminate between pions and electrons with momenta up to 700 MeV/c.

Key words:
PACS: 25.6, 34.8a

1 Introduction

The Bates Large Acceptance Spectrometer Toroid experiment, BLAST, at the MIT-Bates Linear Accelerator Laboratory was designed to study in a systematic manner the spin-dependent electromagnetic interaction in few-nucleon systems at momentum transfers below 1 GeV/c. [1] Utilizing a polarized electron beam; highly polarized, internal gas targets of hydrogen and deuterium; and a symmetric detector configuration: BLAST is able to make simultaneous measurements of several reaction channels for different combinations of beam helicity and target polarization (vector for hydrogen, both vector and tensor for deuterium). BLAST will provide new data on the nucleon and deuteron form factors as well as study few body physics and pion production.

The MIT-Bates linear accelerator consists of a 500 MeV linac with recirculator to produce electrons with energies up to 1 GeV and polarizations of $\sim$ 70%. The BLAST experiment is situated on the South Hall Storage Ring. Injected currents of $\sim$ 175 mA with lifetimes of $\sim$ 25 minutes are typical. A Siberian snake maintains the longitudinal polarization of the stored electron beam and a Compton polarimeter is used to monitor the stored beam polarization. The BLAST detector (Fig. 1) is based on an eight sector, toroidal magnet with a maximum field of $\sim$ 3800 G. The detectors in the left and right, horizontal sectors nominally subtend 20° - 80° in polar angle and $\pm 15^\circ$ azimuthally. The detector is roughly symmetric with each sector containing: wire chambers for charged particle tracking, Cherenkov detectors for electron identification, and time of flight scintillators to measure the relative timing of scattered particles. The neutron detectors are somewhat asymmetric with the right sector having a greater thickness. The data acquisition uses the CODA and trigger supervisor systems from JLAB. This allows multiple triggers to be defined so data can be accumulated for elastic, quasi-elastic, inclusive, and production reactions at the same time. Data are collected reversing the beam helicity each ring fill and randomly cycling through the target spin states every five minutes.

[1] Corresponding author: ricardo.alarcon@asu.edu
[2] Work supported under NSF Awards 0099422 and 0354878.

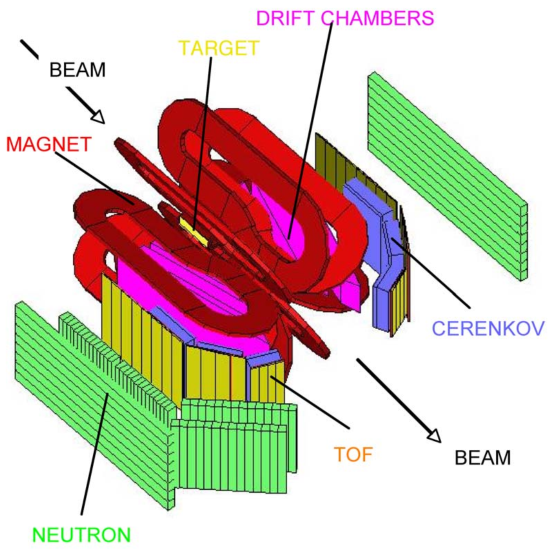

Fig. 1. *A schematic, isometric view of the BLAST detector showing the main detector elements.*

2 Design Considerations

The Cherenkov counters provide the primary electron/pion particle identification for BLAST. The main design considerations are: a uniform, high ($\geq 90\%$) electron detection efficiency; the counters should be compact and minimize energy loss, and they should operate in a region with high ($\approx 100G$) longitudinal magnetic fields. We adopted as a final design an array of counters having silica aerogel as radiator. Aerogel provides a very compact detector in the confined space of BLAST. Fig. 2 shows a schematic of a detector counter and the arrangement in one of the BLAST sectors. There are four counters per sector. The most forward counter contains an aerogel radiator 7 cm thick with an index of refraction n=1.020, the other counters have 5 cm thick aerogel with n =1.030. This arrangement is good enough to discriminate between pions and electrons up to at least 700 MeV/c. Each counter consists of a large box with diffusely reflective walls to collect the Cherenkov light into properly arranged photomultiplier tubes (PMTs).

3 Construction

A complete counter (without the back cover) is shown in Fig. 3. The front and back covers of the light collection boxes were constructed of a 1-inch thick honeycomb panel sandwiched between two thin (1 mm) aluminum plates. The side panels were constructed of 1/8-inch aluminum plates. All the interior surfaces were coated with a white reflective paint specially manufactured for diffusive reflection by Labsphere, Inc. Two identical sets of four counters were constructed, one for each sector of BLAST. Each set consists of a counter at forward angles viewed by 6 PMTs and subtending 20° - 35° , a counter viewed by 8 PMTs and subtending 35° - 50° , and two counters each viewed by 12 PMTs and subtending 50° - 80° (see Fig. 2). All boxes cover the entire azimuthal acceptance of the respective BLAST sector and their dimensions vary slightly due to the magnetic coil shape. The dimensions of the largest boxes were 100 cm wide, 150 cm height, and 19 cm deep. Each counter is fed with a laser pulse for timing and gain monitoring.

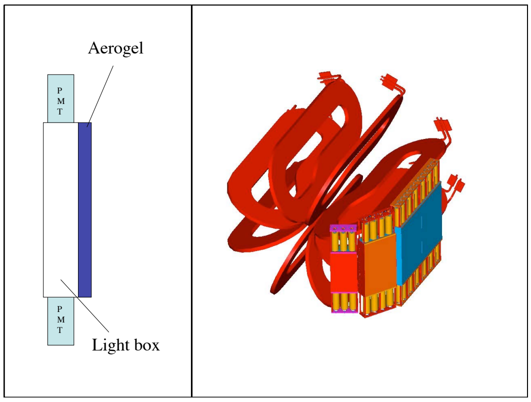

Fig. 2. *Left: schematic side view of one of the Cherenkov counters. Right: arrangement in one of the BLAST sectors.*

For the Cherenkov radiator we used a high transparency aerogel manufactured by Matsushita Electric Works, Ltd. The aerogel comes in tiles of approximately 11 cm by 11 cm with an average thickness of 1 cm. Care in handling the tiles is necessary to avoid chipping the edges. A large counter box contains approximately 580 tiles. The tiles were mounted on top of each other and separated in rows by a stretched, thin mylar foil. Each row was also covered by a similar mylar strip to hold the aerogel in place when the counter is in its vertical position. To properly fit a row sometimes it was necessary to cut the ending tiles which was accomplished with a common razor.

Fig. 3. *A complete Cherenkov counter without the back cover, showing the aerogel, reflective surfaces and one end of PMTs*

The photomultipliers are 5-inch diameter fast tubes (type XP4500B, Photonis). The magnetic shielding for the PMTs consisted of two concentric cylinders of low carbon steel as shown schematically in Fig. 4 . Low carbon steel was chosen because μ-metal shielding saturates at flux densities of more than a few milliteslas. The shielding needs to extend beyond the PMT window for at least one diameter. The configuration shown in Fig. 4 was modeled using the computer code OPERA-3d and it was found that the configuration of an inner tube with a 75 mm radius and 10 mm thick, surrounded by an outer tube with an 88 mm radius and 6 mm thick was the best configuration in order to cancel the longitudinal BLAST fields. Actual dimensions of the shielding tubes were slightly different to accommodate to commercially available tubes. Residual fields of 3-5 Gauss were found when the entire array of Cherenkov counters was operated with the full magnetic field of BLAST which resulted in a significant loss of efficiency for most counters. This was solved by adding iron shielding around the frame that supports the PMTs. To minimize the loss of photons in the entrance region we introduced a simple aluminum cone with a reflectivity of about 98% (see Fig. 4).

A single counter with the dimensions of the larger box was first constructed as a prototype. This unit was tested with cosmic rays and with the electron beam in conjunction with other BLAST detector elements. During the tests the prototype counter performed as expected although it was not possible to test it with the full BLAST magnetic field. The con-

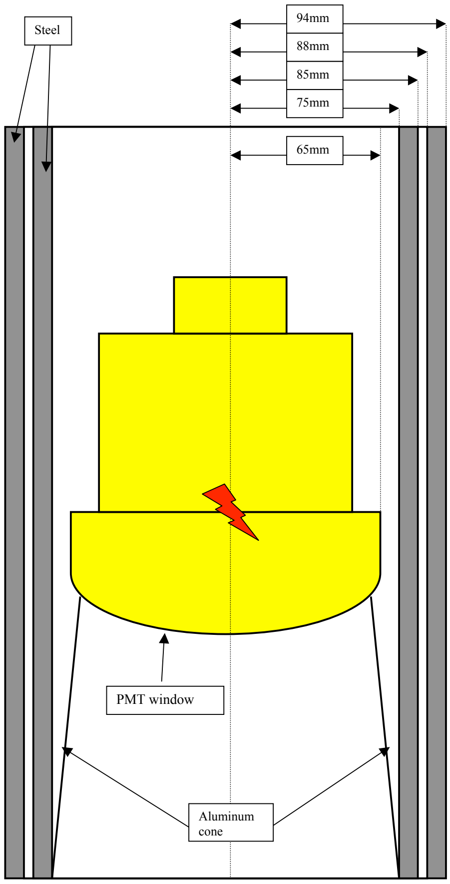

Fig. 4. *A schematic view of a PMT showing the concentric cylinders of soft iron that provide magnetic shielding and the entrance aluminum reflective cone.*

struction of the entire array proceeded with no significant changes from the prototype.

4 Simulations

Initially the above design was modeled using the simulation technique described in Ref. [2]. The corresponding computer code predicts the photoelectron signal, the uniformity of the signal, the average number of PMTs which trigger per event, and the timing resolution of the detector. For BLAST the larger Cherenkov box was modeled and it was found that the counter should produce an average signal of around 4.5 photoelectrons in the absence of an external magnetic field.[1,2]

The photoelectron signal and the average number of

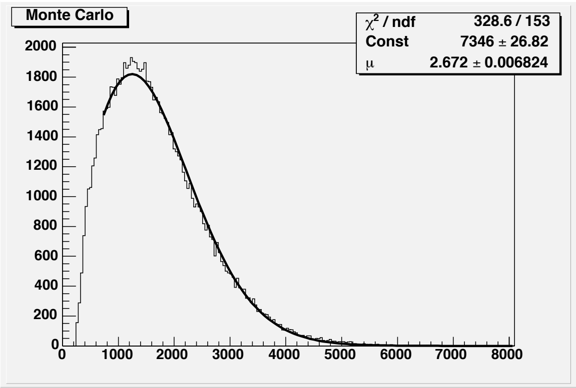

Fig. 5. *A simulated Cherenkov counter ADC event distribution. For the case shown the number of PMTs that fired per event (multiplicity) is four. Also shown is a fit by a Poisson distribution.*

PMTs which trigger per event were used to perform a Monte Carlo simulation of the ADC spectrum for a particular Cherenkov counter. A Poisson event generator [3] was used to simulate the number of photoelectrons and their multiplication throughout the dynode stages in a linear focusing PMT. The Poisson distributed signal takes into account how fluctuations around the mean diminish from the first dynode to the next. This can be expressed by the equation below,

$$\sigma_i = \left[PE \cdot \prod_{j=1}^{m} g_j \right]^{1/2}, m = i - 1, \tag{1}$$

where σ_i is the fluctuation in the distribution of the number of electrons at ith stage, PE is the mean of the photoelectron distribution and g_j's are the gains of the stages which precede the i'th stage. The ADC spectrum for a particular counter was obtained by doing an event by event sum of the individual PMT ADCs that trigger an event. A pedestal-subtracted ADC spectrum produced by the Monte Carlo for a multiplicity of 4 is shown in Fig. 5.

The ADC from the Monte Carlo was fit to the Poisson function with two parameters (Eq. 2); *Const.* which enables the Poisson function to scale itself to the given ADC spectra, and μ which is the mean of the Poisson distribution.

$$y = (Const.) \times \frac{\mu^x e^{-\mu}}{\Gamma[x+1]}, \tag{2}$$

where y is the number of counts per channel, x is the ADC channel, and Γ is the gamma function, given by

$$\Gamma(x) = \int_0^\infty t^{x-1} e^{-t} dt. \tag{3}$$

This function is similar to the one used in Ref. [4]. As seen in Fig. 5 the fit to the ADC has a μ of 2.7 which agrees well with the input number of photoelectrons. In the next section the measured ADC spectra are fitted with this function to extract the number of photoelectrons detected and provide a measurement of the efficiency of the Cherenkov counter.

5 Performance

Preliminary results for the performance of the Cherenkov detectors have been obtained during the on-going measurements with the BLAST detector. By using elastic scattering from hydrogen we have determined the relative efficiency of the Cherenkov counters. The elastic events were selected based on cuts from the reconstructed kinematic variables including coplanarity and timing cuts from the scintillators that are right behind the Cherenkov counters. There are four timing scintillators behind each Cherenkov counter. We have analyzed data for three Cherenkov counters per BLAST sector. The last Cherenkov box in each sector was moved to backward angles, outside the acceptance of the drift chambers, to allow for a measurement of elastic electron-deuteron scattering.

We obtained the relative efficiency polar profile shown in Fig. 6 by counting the number of Cherenkov events that correspond to electron elastic events triggered by a particular scintillator. Results for both left and right BLAST sectors are shown in Fig. 6. Edge effects are noticeable for scintillator 4 and 8. For scintillator 12 there was no significant overlap with the last Cherenkov box for in-bending electrons. Since each scintillator is equipped with a PMT at each end the efficiency has also been studied as a function of position along each scintillator, and it was found to within ±1% of the value shown in Fig. 6.

The ADC distributions of each Cherenkov counter

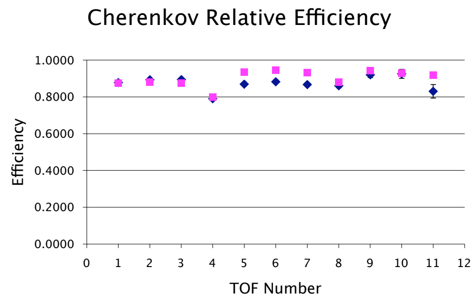

Fig. 6. *An efficiency profile of the Cherekov counters relative to the timing scintillators, corresponding to electrons from electron-proton elastic scattering. For each scintillator two points are shown corresponding to the left and right sector of BLAST respectively. Scintillator 1 corresponds to the most forward angles.*

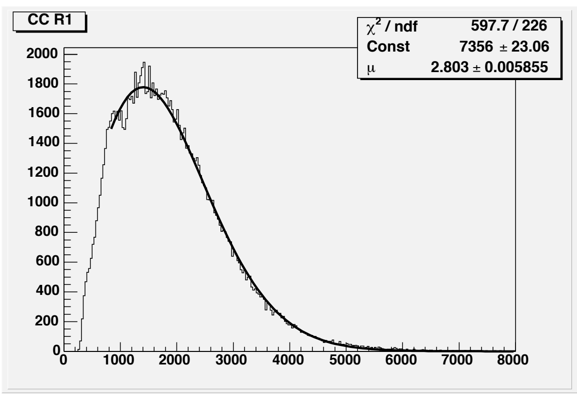

Fig. 7. *Measured ADC distribution for one of the Cherenkov counters corresponding to elastic scattered electrons from hydrogen. The ADC is fitted with the same Poisson distribution of Fig.* **??**

have been fitted with the Poisson function discussed in the previous section. A typical result for one of the large Cherenkov box is shown in Fig. 7. The measured ADC is very similar to that of Fig. 5 indicating a very good agreement between simulation and experimental measurement. The mean of the fitting function yields 2.8 detected photoelectrons per event in a Cherenkov counter which translates into a detection efficiency of 95% well in agreement with the result from Fig. 6.

6 Summary and conclusions

The BLAST Cherenkov detectors consist of two symmetric arrays of diffusely reflective counters with a high transparency aerogel as a radiator. The Cherenkov light is detected by PMTs arranged at each end of a counter. The detectors have been in operation at the Bates Linear Accelerator Center since 2002. The BLAST magnet produces sizable longitudinal magnetic fields at the position of the Cherenkov PMTs. Extra iron shielding to that envisioned in the design was necessary to properly cancel these fields and bring the performance of the counters to expected levels. In addition to electron detection the Cherenkov detectors are used also for background reduction and in triggering electron events in high count rate reactions like inclusive electron scattering. No deterioration in the performance of the Cherenkov counters has been detected.

References

[1] BLAST Technical Design Report, Bates Linear Acc. Center, (1997).

[2] D.W. Higinbotham, Nucl. Instr. And Meth. **A** (1998), no. 414, 332.

[3] W.H. Press et al., *Numerical recipes in fortran 77*, 2 ed., Cambridge University Press, Cambridge, 1992.

[4] L.C. Alexa et al., Nucl. Instr. And Meth. In Phys. Res. **A** (1995), no. 365, 299.